Bonding in Methylalkalimetals $(CH_3M)_n$ (M = Li, Na, K; n = 1, 4). Agreement and Divergences between AIM and ELF Analyses†

Eduard Matito,‡ Jordi Poater,*,§ F. Matthias Bickelhaupt,§ and Miquel Solà*,‡

Institut de Química Computacional and Departament de Química, Universitat de Girona, 17071 Girona, Catalonia, Spain, and Afdeling Theoretische Chemie, Scheikundig Laboratorium der Vrije Universiteit, De Boelelaan 1083, NL-1081 HV Amsterdam, The Netherlands

Received: December 26, 2005; In Final Form: February 11, 2006

The chemical bonding in methylalkalimetals $(CH_3M)_n$ (M = Li−K; n = 1, 4) has been investigated by making use of topological analyses grounded in the theory of atoms in molecules (AIM) and in the electron localization function (ELF). Both analyses describe the C−M bond as an ionic interaction. However, while AIM diagnoses a decrease of ionicity with tetramerization, ELF considers tetramers more ionic. Divergences emerge also when dealing with the bonding topology given by each technique. For the methylalkalimetal tetramers, the ELF analysis shows that each methyl carbon atom interacts through a bond pair with each of the three hydrogen atoms belonging to the same methyl group and through an ionic bond with the triangular face of the tetrahedral metal cluster in front of which the methyl group is located. On the other hand, the AIM topological description escapes from the traditional bonding schemes, presenting hypervalent carbon and alkalimetal atoms. Our results illustrate that fundamental concepts, such as that of the chemical bond, have a different, even colliding meaning in AIM and ELF theories.

1. Introduction

Organometallic species containing polar metal−carbon bonds,[1] such as organolithium, organomagnesium, and organozinc compounds, are important in organic synthesis. They combine in a unique way high reactivity and ease of access. Besides their synthetic utility, they are also of interest because of their unusual geometries that challenge conventional bonding considerations.[2]

Methyl derivatives of organoalkalimetal compounds constitute the simplest organometallic compounds containing the archetype carbon−metal bond, and because of that, they have been analyzed in numerous theoretical[3−9] and experimental[10−15] studies. The high polarity of the alkalimetal−carbon bond present in these compounds results in a partially negatively charged carbon atom, which to an important extent determines the behavior of these compounds as carbon nucleophiles and bases. The carbon−alkalimetal bond is commonly viewed predominantly ionic, with simple ion-pair Coulombic attraction being much more important for the description of the bond than the covalent bonding. This picture has emerged from advanced population analysis methods such as the natural population analysis (NPA), the integrated projected population (IPP) method, or the atoms in molecules (AIM) approach that yield lithium atomic charges between +0.75 to +0.90 e.[3,6,16−18] AIM topological analysis[6,17,19] and modern valence-bond description[20] of the carbon−alkalimetal bond provide further support for the ionic character of this bond. Finally, Streitwieser, Bushby, and Steel have shown that a simple electrostatic model is able to reproduce the ratio of carbon−carbon and lithium−lithium distances in the methyllithium tetramer.[4,21]

As a result, the established idea about this bond is that the electron of the metal is nearly completely transferred to methyl, and covalent interactions play only a marginal role. Nevertheless, there is also some experimental and theoretical evidence of a relevant covalent contribution to the alkalimetal−carbon bond. For instance, the large carbon−lithium NMR coupling constants of up to 17 Hz observed for organolithium aggregates[22] are indicative of the importance of the covalent character of the carbon−lithium bond. Besides, the solubility of simple organolithium compounds in nonpolar solvents has been also considered as a manifestation of the covalent nature of the C−Li bond.[23] Moreover, Streitwieser's aforementioned ideal distance ratio is not found in other similar lithium tetramers such as $(LiH)_4$, $(LiOH)_4$, and $(LiF)_4$, and for the two latter examples an electrostatic model wrongly predicts a planar eight-membered ring structure to be more stable than the tetrahedral structure.[24] In addition, Hirshfeld[25] and Voronoi deformation density[16,26] charge population analyses in methyllithium yield a Li atomic charge of +0.50 and +0.39 e, respectively, pointing out that the charge transfer from Li to the methyl group is far from being complete, i.e., opposite to what is expected for an ionic carbon−lithium bond.[26] Finally, we have recently shown by means of quantitative Kohn−Sham orbital mixing and energy decomposition analyses that the trend in homolytic M−CH_3 bond strength of the MCH_3 species along the series M = Li, Na, K, and Rb is governed by the overlap between the singly occupied molecular orbitals (SOMOs) of the methyl and alkalimetal radicals.[27] These results provide evidence of the importance of the covalent contributions in the C−M bond.

The studies mentioned above show that the nature of the carbon−metal bond in methyl derivatives is interesting and important, but also controversial. In the present work, we reinvestigate the carbon−metal bond by performing atoms in molecules (AIM)[28] and electron localization function (ELF)[29] topological analyses of the $(MCH_3)_n$ species (M = Li, Na, and

† Dedicated to Professor Ramon Carbó-Dorca on the occasion of his 65th birthday.

* To whom correspondence should be addressed. E-mail: miquel@iqc.udg.es.

‡ Universitat de Girona.

§ Scheikundig Laboratorium der Vrije Universiteit.

10.1021/jp057517n CCC: $33.50
Published on Web 03/15/2006

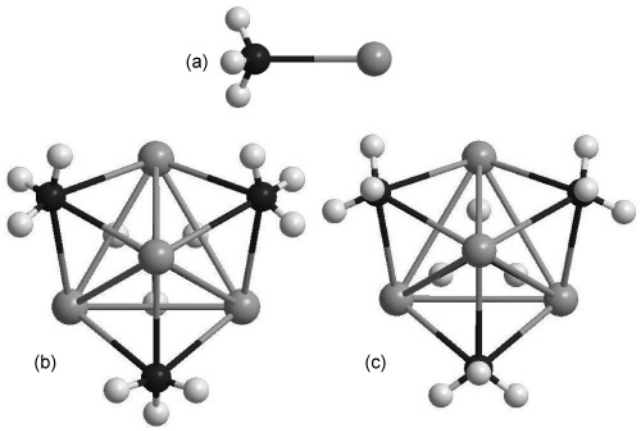

Figure 1. Geometry of the methylalkalimetal monomer (a), the methylalkalimetal tetramer in the staggered conformation (b), and the methylalkalimetal tetramer in the eclipsed conformation (c).

K; $n = 1, 4$) depicted in Figure 1. Our goal is to shed light from yet other perspectives onto the nature of the carbon−metal bond using the complementary approaches of AIM and ELF analyses. Although the AIM study of the electron density for M = Li was already carried out by Ritchie and Bachrach some years ago,[17] and Vidal et al. studied the KCH_3 species with AIM and ELF,[19] in this paper we extend and complement these previous analyses for the full M = Li, Na, and K, $n = 1, 4$ series to discuss the effect of going from Li to the heavier alkalimetals and also the effect of tetramerization. Our AIM results include the localization and delocalization indices[30,31] derived from the second-order density. Moreover, we will provide a comparison between the AIM and ELF descriptions of the bonding in these species. Here we anticipate that, not unexpectedly, both AIM and ELF yield a picture of the carbon−alkalimetal bond that is highly polar. Interestingly, however, the two models disagree regarding a number of fundamental bonding descriptors. Implications of these findings are discussed.

2. Methodology

2.1. AIM and ELF Topological Theories. The partitioning of the molecular space into basins of attractors allows the calculation of several properties by integration over these basins. In the atoms in molecules (AIM)[28,32−34] theory, the basins are defined as a region in the Euclidean space bounded by a zero-flux surface in the gradient vectors of the one-electron density, $\rho(\mathbf{r})$, or by infinity. In this way, a molecule is split into its constituent atoms (atomic basins) and, if present, nonnuclear attractors, using only the one-electron density distribution. Such a division of the topological space is exhaustive, so that many molecular properties, e.g. energy, dipole moments, electron populations, etc., can be written as the sum of atomic contributions. A different partitioning of the space was proposed in 1990 by Becke and Edgecombe[35] using a local scalar function, the electron localization function (ELF) denoted by $\eta(\mathbf{r})$, which is related to the Fermi hole curvature. As shown by Savin et al.,[29] the ELF measures the excess of kinetic energy density due to the Pauli repulsion. In the region of space where the Pauli repulsion is strong (single electron or opposite spin-pair behavior) the ELF is close to one, whereas where the probability of finding the same-spin electrons close together is high, the ELF tends to zero. For an N-electron single determinantal closed-shell wave function built from Hartree−Fock (HF) or Kohn−Sham orbitals, ϕ_j, the ELF function is given by:[36]

$$\eta = \frac{1}{1 + \left(\frac{D}{D_h}\right)^2} \tag{1}$$

where

$$D = \frac{1}{\rho}\nabla_2^2\Gamma^{(2)\sigma\sigma}(\vec{r}_1,\vec{r}_2) = \frac{1}{2}\sum_{j=1}^{N}|\nabla\phi_j|^2 - \frac{1}{8}\frac{|\nabla\rho|^2}{\rho} \tag{2}$$

$$D_h = \frac{3}{10}(3\pi^2)^{2/3}\rho^{5/3} \tag{3}$$

$$\rho = \sum_{j=1}^{N}|\phi_j|^2 \tag{4}$$

and where N is the number of electrons and $\Gamma^{(2)\sigma\sigma}(\vec{r}_1,\vec{r}_2)$ is one of the same-spin contributions to the second-order density, $\Gamma^{(2)}(\vec{r}_1,\vec{r}_2)$. As the ELF is a scalar function, the analysis of its gradient field can be carried out in order to locate its attractors (local maxima) and the corresponding basins. There are basically two chemical types of basins, core (C) and valence (V), that are characterized by their synaptic order, which is the number of core basins with which they share a common boundary.[37] Graphical representations of the bonding are obtained by plotting isosurfaces of the ELF which delimit volumes within which the Pauli repulsion is rather weak. The localization domains are called irreducible when they contain only one attractor and are called reducible otherwise. The reduction of reducible domains is another criterion of discrimination between basins, and the reductions occur at a critical value of the bonding isosurface. The domains are ordered with respect to the ELF critical values, yielding bifurcations (tree diagrams).

The partitioning of the molecular space enables basin-related properties to be calculated by integrating the density of a certain property over the volume of the basins. Thus, for a basin labeled Ω_i, one can define the average population as:

$$\bar{N}(\Omega_i) = \int_{\Omega_i}\rho(\vec{r})d\vec{r} \tag{5}$$

and its variance:

$$\sigma^2(\Omega_i) = \langle(N(\Omega_i) - \bar{N}(\Omega_i))^2\rangle = \int_{\Omega_i}\Gamma^{(2)}(\vec{r}_1,\vec{r}_2)d\vec{r}_1 d\vec{r}_2 - \bar{N}(\Omega_i)[\bar{N}(\Omega_i) - 1] \tag{6}$$

The variance is a measure of the quantum mechanical uncertainty of the basin population, which can be interpreted as a consequence of the electron delocalization. Equation 6 can be written in terms of the exchange-correlation density, $\Gamma_{XC}(\vec{r}_1,\vec{r}_2)$, as:

$$\sigma^2(\Omega_i) = \int_{\Omega_i}\Gamma_{XC}(\vec{r}_1,\vec{r}_2)d\vec{r}_1 d\vec{r}_2 + \bar{N}(\Omega_i) = \bar{N}(\Omega_i) - \lambda(\Omega_i) \tag{7}$$

where $\lambda(\Omega_i)$ is the so-called localization index (LI), so that we can see the variance $\sigma^2(\Omega_i)$ is nothing but a measure of total electron delocalization into the basin Ω_i.[38] Besides, the relative fluctuation parameter introduced by Bader[30,39] indicates the

relative electronic delocalization of a particular atomic basin:

$$\lambda_F(\Omega_i) = \frac{\sigma^2(\Omega_i)}{\bar{N}(\Omega_i)} \quad (8)$$

which is positive and expected to be less than one in most cases. It is important noticing the difference between this quantity and the LI in eq 7. While $\lambda_F(\Omega_i)$ is a fluctuation parameter that stands for the ratio of electrons delocalized, the latter is a measure of the number of electrons localized into the basin Ω_i. It is always less than the corresponding atomic population, $N(\Omega_i)$, except for totally isolated atoms, where there is no exchange or correlation with electrons in other atoms.

The variance, $\sigma^2(\Omega_i)$, can also be spread in terms of contributions from other basins, the covariance, $V(\Omega_i,\Omega_j)$, which has a clear relationship with the so-called delocalization index (DI), $\delta(\Omega_i,\Omega_j)$:

$$V(\Omega_i,\Omega_j) = \langle N(\Omega_i)\cdot N(\Omega_j)\rangle - \langle N(\Omega_i)\rangle\langle N(\Omega_j)\rangle = \int_{\Omega_i}\int_{\Omega_j}(\Gamma^{(2)}(\vec{r}_1,\vec{r}_2) - \rho(\vec{r}_1)\rho(\vec{r}_2))d\vec{r}_1 d\vec{r}_2 = \int_{\Omega_i}\int_{\Omega_j}\Gamma_{XC}(\vec{r}_1,\vec{r}_2)d\vec{r}_1 d\vec{r}_2 = -\frac{\delta(\Omega_i,\Omega_j)}{2} \quad (9)$$

The DI, $\delta(\Omega_i,\Omega_j)$, accounts for the electrons delocalized or shared between basins Ω_i and Ω_j.[31] As the total variance in a certain basin can be written in terms of covariance, we have:

$$\sigma^2(\Omega_i) = -\sum_{j\neq i} V(\Omega_i,\Omega_j) = \sum_{j\neq i}\frac{\delta(\Omega_i,\Omega_j)}{2} \quad (10)$$

From this quantity above one can do the usual contribution analysis (CA), listed on the tables as a percentage:

$$CA(\Omega_i|\Omega_j) = \frac{V(\Omega_i,\Omega_j)}{\sum_{k\neq j} V(\Omega_j,\Omega_k)}\times 100 = -\frac{V(\Omega_i,\Omega_j)}{\sigma^2(\Omega_j)}\cdot 100 \quad (11)$$

The contribution analysis gives us the main contribution arising from other basins to the variance, i.e., the delocalized electrons of basin Ω_j on basin Ω_i, giving us a measure of electron pair sharing between two regions of the molecular space.

It is worth noting that for closed-shell molecules and for single determinant wave functions, LIs and DIs can be written in terms of the integrals $S_{kl}(\Omega_i)$, i.e., the overlap between molecular spin-orbitals k and l in a basin Ω_i as:[31]

$$\lambda(\Omega_i) = \sum_{k,l}(S_{kl}(\Omega_i))^2 \quad (12)$$

$$\delta(\Omega_i,\Omega_j) = 2\sum_{k,l} S_{kl}(\Omega_i)S_{kl}(\Omega_j) \quad (13)$$

where the summations run over all the occupied molecular spin-orbitals. The accuracy of eqs 12 and 13 for computing LIs and DIs at the HF level has been discussed in a previous work.[40] Finally, using eqs 7−10 it can be proved that the following relations between LIs and DIs and variance, covariance, and average populations exist:

$$N = \sum_i \lambda(\Omega_i) + \frac{1}{2}\sum_i\left(\sum_{j\neq i}\delta(\Omega_i,\Omega_j)\right) = \sum_i (N(\Omega_i) - \sigma^2(\Omega_i)) - \sum_i\left(\sum_{j\neq i} V(\Omega_i,\Omega_j)\right) = \sum_i N(\Omega_i) \quad (14)$$

Quantities such as DIs, variances and covariances have been used to discuss the degree of ionicity/covalency of a given bond,[31,41] and they will be applied to our systems. Moreover, within the framework of the AIM theory, the magnitude of the density ($\rho(\mathbf{r}_{bcp})$), of the Laplacian of the density ($\nabla^2\rho(\mathbf{r}_{bcp})$), and of the ratio between the perpendicular and the parallel curvatures at the bond critical point ($|\lambda_1|/\lambda_3$) have been previously applied in order to classify an interaction as either ionic or covalent, or having an intermediate character.[28,32,33,42,43] Thus, a clearly ionic interaction (i.e. LiF) would be characterized by the above parameters as: $|\lambda_1|/\lambda_3 < 1$, $\rho(\mathbf{r}_{bcp})$ small, and $\nabla^2\rho(\mathbf{r}_{bcp}) > 0$; and a clearly covalent interaction (i.e. N_2) as: $|\lambda_1|/\lambda_3 > 1$, $\rho(\mathbf{r}_{bcp})$ large, and $\nabla^2\rho(\mathbf{r}_{bcp}) < 0$. Finally, the energy density at the bond critical point, $H(\mathbf{r}_{bcp})$, which is equal to the sum of the potential and kinetic energy densities, has been also used to characterize chemical bonds:[33] a negative value of $H(\mathbf{r}_{bcp})$ indicates that the potential energy dominates, thus denoting a concentration of charge and a covalent bond, while for positive values the kinetic energy is more important, implying a closed-shell interaction.

2.2. Computational Details. Molecular geometries for all the methylalkalimetals have been fully optimized at the HF/6-311G** level of theory by means of the Gaussian 98 program.[44] For comparison purposes, monomers have also been calculated at the CISD/6-311G** level of theory. All stationary points found have been characterized as either minima or n^{th}-order saddle points by computing the vibrational harmonic frequencies; n^{th}-order saddle points have n imaginary frequencies while for minima all frequencies are real. The wave functions and electron densities required to carry out the AIM and ELF topological analyses have also been obtained at the same level of theory using the Gaussian 98 program. Although Density Functional Theory (DFT) performs somehow better for these systems,[27] the HF method has been chosen because within DFT the calculation of LIs and DIs is problematic. The reason is that the second-order density is not available at the DFT level and must be approximated using a HF-like expression.[40] However, HF reproduces qualitative features of trends in geometry and energy correctly. For each molecule, a topological analysis of $\rho(\mathbf{r})$ has been performed and electron populations (N) have been obtained for each atom, using the AIMPAC package of programs.[45] For the monomers calculated with CISD/6-311G** method, DIs and LIs have been computed at the same level of theory using the approximation suggested by Wang and Werstiuk.[46] The numerical accuracy of the AIM calculations has been assessed using two criteria: (i) The integration of $\nabla^2\rho(\mathbf{r})$ within an atomic basin must be close to zero; (ii) The number of electrons in a molecule must be equal to the sum of all atom populations of a molecule and also equal to the sum of all the LIs and DIs in the molecule according to eq 14. For all the atomic calculations, integrated values of $\nabla^2\rho(\mathbf{r})$ were always less than 0.001 au. For all the molecules, errors in calculated number of electrons were always less than 0.01 au. In addition, a visual analysis of the critical points has been carried out by means of the AIM2000 software.[47] The Gaussian 98[44] wave function output was also treated with the TopMod package[48] in

TABLE 1: HF/6-311G (first row), CISD/6-311G** (second row in parentheses), and mm-wave Gas Phase (third row in brackets) Geometrical Parameters of the Methylalkalimetal Monomers. Distances Are Given in Angstroms (Å) and Angles in Degrees**

molecule	R(C−M)	R(C−H)	∠MCH	∠HCH
CH_3Li	1.985	1.095	112.8	105.9
	(1.981)	(1.100)	(112.8)	(105.9)
	[1.959][a]	[1.111][a]		[106.2][a]
CH_3Na	2.341	1.092	111.5	107.4
	(2.335)	(1.098)	(111.5)	(107.3)
	[2.299][a]	[1.091][a]		[106.0][a]
CH_3K	2.718	1.097	112.8	106.0
	(2.674)	(1.099)	(112.9)	(105.9)
	[2.633][b]	[1.135][b]		[107.0][b]

[a] Results from ref 12. [b] Results from ref 10.

order to perform the ELF analysis. The Vis5d program[49] was used for the visualization of the ELF.

3. Results and Discussion

The present section is divided into two subsections. The first one takes into account the methylalkalimetal monomers, and the second one considers the tetramers. For each section, the molecular structures and the AIM and ELF analyses will be discussed with special emphasis on the question to what extent the AIM and ELF topological descriptions agree and where they yield colliding or differing pictures.

3.1. Methylalkalimetal Monomers. *Structures.* Table 1 summarizes the structural parameters obtained at the HF/6-311G** and CISD/6-311G** levels of theory for the three methylalkalimetal monomers studied: CH_3Li, CH_3Na, and CH_3K. As it can be seen, the HF/6-311G** C−M bond distance increases when descending the periodic table from 1.985 (Li), to 2.341 (Na), and to 2.718 Å (K). The C−H bond distance is quite invariant and amounts to ca. 1.10 Å throughout the series. Meanwhile, the ∠MCH angles are also kept quite constant for the three monomers (111−112°), not varying the pyramidalization of these C_{3v} symmetric structures when going down the periodic table. This is also observed for the ∠HCH angles, which are almost constant (106−107°).

The above HF/6-311G** geometrical parameters reasonably agree with CISD/6-311G** results and previous theoretical studies[7−9,16,27] as well as microwave experiments,[10,12] which also yield a monotonic increase of the C−M bond along CH_3Li, CH_3Na, and CH_3K. Actually, the experimental C−M bond lengths (1.959,[12] 2.299,[12] and 2.633 Å[10] for Li, Na, and K, respectively) are systematically shorter, by 2−3%, than our theoretical values. Thus, just focusing on this series of molecules, the optimization at the HF/6-311G** level of theory can be considered satisfactory, achieving structural data quite similar to that yielded by more expensive methods, like the CISD or the CCSD(T) levels of theory.[8] Metal fluoride distances are also well reproduced at the HF level.[50]

AIM Analysis. Table 2 contains the most important properties obtained from the AIM analysis. It is worth noting that an AIM analysis of CH_3Li species at the HF/6-311G** level has been already reported by Ponec and co-workers.[6] Here, we complement their analysis by comparing the results obtained for CH_3Li with those of CH_3Na and CH_3K. The metal atomic charges for the three monomers are: +0.914 (Li), +0.799 (Na), and +0.844 (K) electrons, suggesting the picture of a metal cation bound to a carbanion. The charge separation across the C−M bond in methylalkalimetal monomers decreases from Li to Na and increases from Na to K. This behavior has been already previously observed and traced to the interplay of two effects: the increasing polarity of the C−M bond when going from Li to Na is overcompensated by the reduction of the participation of the alkalimetal np_σ atomic orbital.[27] Thus, from the AIM metal charges, we could conclude that these monomers are highly (80−90%) ionic systems. However, as pointed out earlier,[26,27] atomic charges are very dependent on the scheme of calculation employed, and, as a consequence, they cannot be used as absolute bond polarity indicators.

TABLE 2: HF/6-311G (CISD/6-311G** given in parentheses) Atomic Populations (N), Atomic Charges (q), Localization Indices (λ), Localization Percentages (%λ), and Delocalization Indices (δ) Obtained from the AIM Analysis for the Methylalkalimetal Monomers. Units Are Electrons**

molecule	atom	N	q	λ	%λ	pair	δ(A,B)
CH_3Li[a]	C	6.578	−0.578	4.900	74.5	C,Li	0.177
		(6.691)	(−0.691)	(5.222)	(78.1)		(0.180)
	Li	2.086	0.914	1.986	95.2	C,H	1.060
		(2.091)	(0.909)	(1.990)	(95.2)		(0.919)
	H	1.112	−0.112	0.521	46.9	H,H′	0.057
		(1.073)	(−0.073)	(0.565)	(52.7)		(0.044)
						CH_3,Li	0.198
							(0.202)
CH_3Na	C	6.466	−0.466	4.700	72.7	C,Na	0.360
		(6.560)	(−0.560)	(5.013)	(76.4)		(0.352)
	Na	10.201	0.799	9.996	98.0	C,H	1.057
		(10.223)	(0.777)	(10.021)	(98.0)		(0.914)
	H	1.111	−0.111	0.518	46.6	H,H′	0.056
		(1.072)	(−0.072)	(0.563)	(52.5)		(0.044)
						CH_3,Na	0.411
							(0.352)
CH_3K	C	6.429	−0.429	4.677	72.8	C,K	0.328
		(6.491)	(−0.491)	(4.924)	(75.9)		(0.353)
	K	18.156	0.844	17.968	99.0	C,H	1.058
		(18.191)	(0.809)	(17.988)	(98.9)		(0.928)
	H	1.138	−0.138	0.540	47.5	H,H′	0.061
		(1.106)	(−0.106)	(0.584)	(52.8)		(0.049)
						CH_3,K	0.376
							(0.408)

[a] Some of these results can be found in ref 6.

Table 3 contains additional parameters derived from the first-order density from a Bader's theory point of view. From the results in Table 3, it is seen that for all three cases the parameters obtained are $|\lambda_1|/\lambda_3 < 1$, $\rho(\mathbf{r}_{bcp})$ small, $\nabla^2\rho(\mathbf{r}_{bcp}) > 0$, and $H(\mathbf{r}_{bcp}) > 0$. These values suggest that the C−M interaction in methylalkalimetal monomers is a typical closed-shell (electrostatic) interaction, and, indeed, they are not far from those found for the alkalimetal fluorides (see Table 3). In contrast, for a polar covalent bond such as the C−F bond in CH_3F, the values of $\rho(\mathbf{r}_{bcp})$ are relatively large and $H(\mathbf{r}_{bcp}) < 0$, as it can be seen in Table 3. According to the $\rho(\mathbf{r}_{bcp})$ and $\nabla^2\rho(\mathbf{r}_{bcp})$ values, the ionicity of the C−M bond increases when going from Li to K, as expected from the metal electronegative differences. Finally, Table 2 gathers LIs and DIs extracted from the second-order density, together with the localization percentages (%λ), which for comparison along the series Li to K are even more valuable than the LIs. The large values of the localization percentages in the alkalimetal are also expected for a closed-shell interaction. Descending along the first column of the Periodic Table, the metal %λ increases from 95.2% (Li) to 99.0% (K), in line with the C−M bond increase of ionicity. The low δ(C,M) delocalization indices are also consistent with a predominantly ionic C−M bond. However, in contrast to $\rho(\mathbf{r}_{bcp})$, $\nabla^2\rho(\mathbf{r}_{bcp})$, and %λ, DIs increase when going from Li (0.177 e) to Na (0.360 e), and slightly decrease from Na to K (0.328 e). This tendency is also observed if we take into account the methyl group as a lonely entity, as it can be seen from the $\delta(CH_3,M)$ values (Li 0.198 e; Na 0.411 e; K 0.376 e), and also if we fix the same

TABLE 3: HF/6-311G Density Values ($\rho(r_{bcp})$), Laplacian of the Density Values ($\nabla^2\rho(r_{bcp})$), Ratio Values between the Perpendicular and the Parallel Curvatures ($|\lambda_1|/\lambda_3$), and Local Energy Density ($H(r_{bcp})$) at the Bond Critical Point of the C−M Bond for the Methylalkalimetal Monomers and Tetramers. For Comparison, the Same Quantities Are Given for the M−F Bonds in Alkalimetal Fluorides and the C−F Bond of CH_3F. All Quantities Are Given in au**

molecule	$\rho(r_{bcp})$	$\nabla^2\rho(r_{bcp})$	λ_1	λ_2	λ_3	$\lvert\lambda_1\rvert/\lambda_3$	$H(r_{bcp})$
CH_3Li	0.0441	0.2180	−0.0634	−0.0634	0.3446	0.1840	0.00143
CH_3Na	0.0330	0.1500	−0.0336	−0.0336	0.2172	0.1546	0.00235
CH_3K	0.0293	0.0928	−0.0247	−0.0247	0.1422	0.1736	0.00187
$(CH_3Li)_4$ ecl	0.0229	0.1140	−0.0277	−0.0271	0.1688	0.1638	0.00453
$(CH_3Na)_4$ ecl	0.0155	0.0728	−0.0158	−0.0157	0.1041	0.1521	0.00268
$(CH_3K)_4$ stg	0.0143	0.0488	−0.0112	−0.0093	0.0692	0.1618	0.00148
LiF	0.0701	0.7224	−0.1616	−0.1616	1.0457	0.1545	0.0274
NaF	0.0486	0.4300	−0.0767	−0.0767	0.5832	0.1315	0.0156
KF	0.0475	0.2844	−0.0577	−0.0577	0.3999	0.1443	0.0059
CH_3F	0.2351	0.5336	−0.3984	−0.3984	1.3302	0.3000	−0.2993

TABLE 4: HF/6-311G ELF Values at Attractors (η), Basin Populations ($N(\Omega_i)$), Standard Deviations ($\sigma^2(\Omega_i)$), Relative Fluctuations ($\lambda_F(\Omega_i)$), and Contributions of the Other Basins (%) to $\sigma^2(\Omega_i)$, Obtained for the Methylalkalimetal Monomers**

molecule	Ω	η	$N(\Omega_i)$	$\sigma^2(\Omega_i)$	$\lambda_F(\Omega_i)$	contribution analysis
CH_3Li	C(C)	0.13	2.05	0.24	0.12	28%V(C), 24%V(C,H_i)
	C(Li)	0.09	2.00	0.07	0.03	71%V(C), 10%V(C,H_i)
	V(C,H_i)	0.80	1.97	0.68	0.34	36%V(C), 27%V(C,H_i), 9%C(C)
	V(C)	0.80	2.01	0.85	0.42	28%V(C,H_i), 8%C(Li), 8%C(C)
CH_3Na	C(C)	0.13	2.05	0.24	0.12	28%V(C), 24%V(C,H_i)
	C(Na)	0.05	10.04	0.13	0.01	77%V(C), 8%V(C,H_i)
	V(C,H_i)	0.80	1.99	0.68	0.34	35%V(C), 27%V(C,H_i), 9%C(C)
	V(C)	0.80	1.92	0.89	0.46	27%V(C,H_i), 11%C(Na), 8%C(C)
CH_3K	C(C)	0.15	2.07	0.24	0.12	28%V(C), 24%V(C,H_i)
	C(K)	0.05	18.06	0.16	0.01	79%V(C), 7%V(C,H_i)
	V(C,H_i)	0.79	1.97	0.67	0.34	36%V(C), 27%V(C,H_i), 9%C(C)
	V(C)	0.79	1.92	0.90	0.47	27%V(C,H_i), 12%C(K), 8%C(C)

∠MCH pyramidalization angle for the three methylalkalimetal monomers. Thus, instead of δ(C,M) decreasing when descending the Periodic Table due to the C−M bond being more ionic, we observe the opposite trend found for the atomic charges, i.e., δ(C,Li) < δ(C,Na) > δ(C,K). In fact, the trend in DIs is governed by the atomic charges, as a consequence of the following relationship derived from eq 14:

$$N(\Omega_i) = \lambda(\Omega_i) + \frac{1}{2}\sum_{j\neq i}\delta(\Omega_i,\Omega_j) \qquad (15)$$

According to eq 15, a lower positive atomic charge on the metal corresponds to larger atomic populations, and because the LIs are almost equal to the number of core electrons for all systems, this goes with a bigger $N(\Omega_i) - \lambda(\Omega_i)$ difference, thus implying a larger δ(C,M) value (the δ(H,M) values are similar and close to zero for all MCH_3 systems studied). This explains the larger δ(C,Na) in $NaCH_3$ as compared to δ(C,Li) in $LiCH_3$. Very recently, Vidal, Melchor, and Dobado[19] have studied the CH_3K system at the DFT level by means of AIM and ELF techniques, also attributing a clear ionic character to the C−K bond. In addition, from Fermi hole analyses, Ponec et al.[6] have also concluded that the C−Li bonds in CH_3Li are predominantly ionic. Finally, to demonstrate the validity of the above HF results, values for AIM analysis at the CISD/6-311G** level of theory are also shown in Table 2. As one can see, they are pretty close to HF ones, especially those concerning the DIs of the polar C−M bonds, stressing once again the adequacy of the HF calculations reported. The DIs of the covalent C−H bonds are somewhat smaller when correlation is included as expected from previous studies.[40,46]

ELF Analysis. The ELF method represents an interesting alternative to AIM in order to analyze chemical bonding in molecules and solids.[29,51] The results obtained from the ELF method for methyllithium, -sodium, and -potassium are summarized in Table 4. In all three cases there are two core attractors, labeled C(C) and C(M), and corresponding to carbon and metal core electrons, respectively; three protonated disynaptic attractors, V(C,H_i), which represent the three C−H bonds, and one monsynaptic attractor, V(C), associated to the valence electrons of the carbon atom. As a general trend, for the three metals, the C(C) basins present populations slightly larger than 2 (∼2.05 e); the C(M) basin populations are 2.00, 10.04, and 18.06 for Li, Na, and K, respectively, which are the expected values for the core part of each metal atom. With respect to the valence basins, V(C,H_i) basin populations are slightly lower than 2, the typical value for the single bond in a Lewis sense. The reason for the so marked pairing of electrons is the condition provided by the ELF, that seeks for regions on the molecular space where the probability of finding a couple of electrons is higher. And finally, the presence of the V(C) basin and the lack of a valence basin associated with both atoms, V(C,M),[51] indicates the existence of an unshared-electron interaction[29,52] between the metal and the methyl group. This V(C) basin can be attributed to the nonbonding electron density in the valence shell of the C, at close distance to the core C(C) basin. Further, there is no monosynaptic V(M) basin, which implies a transfer of the electron density of the valence shell of the metal to the methyl group. This view is supported by the V(C) populations, N(V(C)), close to two. Thus, for these three systems, the average number of electrons per basin, obtained by integration of the electron density function over the basins, corresponds roughly to the number of electrons expected on chemical grounds for an ionic system. The above classification of basins is very similar to that found for the MCCH (M = Li, Na, K) systems analyzed by Mierzwicki et al.,[53] which also lack the disynaptic V(C,M) basin.

To study the electronic delocalization of each basin, as previously done in the AIM analysis, it is useful to analyze the relative fluctuation parameter, $\lambda_F(\Omega_i)$, calculated from eq 8. The core basins present very low relative fluctuation values, especially the metal core basins, λ_F(C(C)) = 0.12 and λ_F(C(M))

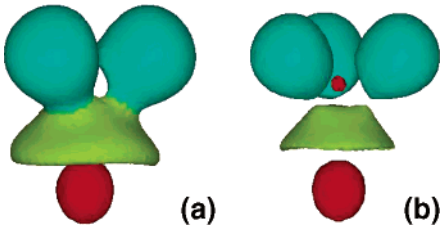

Figure 2. ELF isosurface of the methyllithium monomer with η values of 0.60 (a) and 0.80 (b). The color scale code used for the localization domain is as follows: core, red; valence protonated, green; valence disynaptic, yellow.

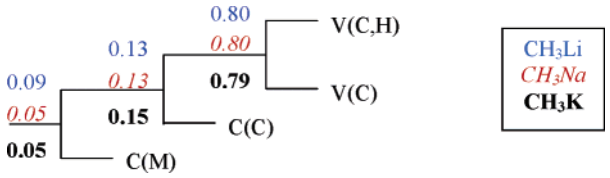

Figure 3. Localization domain reduction tree-diagram of methylalkalimetal monomers CH_3M with M = Li, Na, and K.

$\approx$ 0.01−0.03, showing the high localization of these electrons, while the protonated disynaptic valence basins present a higher constant relative fluctuation (0.34) for the three monomers, showing the similar character of this bond. And finally, the relative fluctuation corresponding to the V(C) basin is even higher and increases when descending the periodic table from 0.42 (Li), to 0.46 (Na), and to 0.47 (K). These fluctuations must be complemented with the contribution percentages of other basins to $\sigma^2(\Omega_i)$. If we focus on the V(C) basin, the most electronically spread, it is seen how the protonated disynaptic basins account for most of the total population variance of this basin ($3 \times 27-28\% \approx 80\%$). The rest of the contribution mainly comes from the core basin of the carbon atom, which remains quite constant (8%), and also from the core basin of the metal atom, whose percentage increases with the size of the alkalimetal, as expected. This low contribution from the C(M) to the V(C) reinforces the ionic nature of the C−M bond.

From a more qualitative point of view, Figure 2 contains an ELF isosurface plot for methyllithium, where it is possible to distinguish the C(M), C(C), V(C,H_i), and V(C) basins. As the attractor V(C) is close to the core region of the C and it only circumscribes the carbon core at low ELF η values ($\eta \approx 0.1$), this bonding situation can be described as ionic.[29] The ELF isosurface plots for methylsodium and methylpotassium are not included as being visually equivalent. In addition, the bifurcation graph (see Figure 3 and η values in Table 5) provides a hierarchy that is consistent with the relative fluctuation values. It must be mentioned that all three systems present almost the same bifurcation graph with the corresponding ELF values. Thus, the C(M) basin is the first one to be partitioned, $\eta \approx 0.05-0.09$, followed by C(C), with $\eta \approx 0.13-0.15$, and it is not till $\eta \approx 0.80$ that the valence basin is split into V(C,H_i) and V(C) basins. It is worth mentioning that if we strictly apply the conditions given by Savin et al.[37] to decide whether a valence attractor is connected to a core attractor or not, the conclusion about the nature of the V(C) basin and the C−M bond would change. The frontier between ionicity and polar covalency was proposed for bifurcation values of $\eta \approx 0.02$ for the C(M) basin. Since in our systems the bifurcation occurs at $\eta \approx 0.05-0.09$, then according to this criterion, we would have a V(C,M) basin and a polar covalent C−M bond, especially for CH_3Li. However, we consider that the Savin et al. criterion[37] is probably too strict (for instance, for LiF the bifurcation occurs at 0.05, and a threshold spectrum of $\eta \approx 0-0.1$ instead of a sharp cutoff seems to be more reasonable). Finally, in agreement with AIM analysis, the ELF results (η, σ^2, N, λ_F) also show that the C−Na bond resembles C−K rather than C−Li.

From the relative fluctuation values together with the bifurcation graph above, we can attribute an ionic character to the C−M bond. Thus, both AIM and ELF analyses agree that the C−M bond is highly polar and associated with ionic bonding.

3.2. Methylalkalimetal Tetramers. *Structures*. All methylalkalimetal tetramers $(CH_3M)_4$ have T_d symmetry and consist of a tetrahedral cluster of alkalimetal atoms surrounded by four methyl groups, one on each M_3 face, oriented with respect to the latter either eclipsed or staggered (see Figure 1). The structure looks more or less like a distorted cube, as it can be seen in Figure 4. Depending on the size of the alkalimetal it looks more like two tetrahedrons, the inner tetrahedron pointing with its vertexes to the faces of the outer one.

Table 5 summarizes the different geometrical parameters optimized at the HF/6-311G** level of theory of the distorted cube structures for the three methylalkalimetal tetramers studied, considering the two possible spatial conformations: staggered and eclipsed for each of them. Tetramerization, i.e., going from the monomer to the tetramer, causes the C−M bond to elongate substantially by 0.2−0.3 Å, whereas the C−H bond distance increases only slightly by 0.01 Å. The distortion of the cube can be measured by means of the α and β angles (see Figure 4) and the dihedral angle of a cube side, ∠CMCM, which decreases when descending the periodic table, thus getting closer to a regular cube for M = K. There is also a remarkable increase in pyramidalization of the methyl group as follows from the ∠HCH angle, which decreases by 3° for lithium and up to 5° for the heavier alkalimetals.

With respect to the eclipsed conformation, the C−M bond distance increases monotonically when descending the periodic table, from 2.211 (Li), to 2.613 (Na), and to 3.024 Å (K). The M−M bond distances also increase from Li to Na by about 0.6 Å and from Na to K by 0.4 Å. As previously observed for the monomers, the C−H bond distance is kept quite constant at 1.10 Å, as well as the extent of pyramidalization of the methyl groups with ∠HCH angles of about 102−103°. Compared to the eclipsed conformation, for the staggered one, the C−H bonds are only marginally shorter (by 0.001 Å), and the methyl groups slightly less pyramidal (∠HCH angle increases by less than 2°), mainly because of the steric repulsion of the metal on the hydrogen atoms. Our HF/6-311G** molecular structures are in good agreement with the existing crystal structures (see Table 5).

Finally, according to the relative energies obtained for the tetramers studied in both conformations, listed in Table 5, the eclipsed form is the most stable for methyllithium and -sodium tetramers, whereas the staggered form is the most stable for methylpotassium tetramer. Here, it must be mentioned that crystal structures of the three tetramers taken into study always yield the staggered conformation of the methyl groups with respect to the M_3 face to which they are coordinated, whereas we find the eclipsed orientation to be the lowest-energy structure for M = Li and Na.[9] Intermolecular interactions and crystal packing may be responsible for the staggered conformation observed experimentally for the methyllithium and -sodium tetramers. The HF/6-311G** frequency analysis shows that the two Na conformers and the most stable form for the Li and K tetramers are minima, whereas the Li tetramer in its staggered form and the K tetramer in its eclipsed conformation are fourth-order saddle points with a four times degenerate imaginary frequency.

TABLE 5: HF/6-311G Relative Energy and Geometrical Parameters of the Eclipsed and Staggered Methylalkalimetal Tetramers. Relative Energies Are Given in kcal·mol^{-1}, Distances in Angstroms (Å), and Angles in Degrees[a,b]**

	$(CH_3Li)_4$		$(CH_3Na)_4$		$(CH_3K)_4$	
	ecl	stg	ecl	stg	ecl	stg
ΔE	0.00	4.15	0.00	1.79	0.0	−3.05
R(C,M)	2.211	2.224 [2.256(6)][c]	2.613	2.602 [2.57−2.68][d]	3.024	2.978 [2.947(2), 3.017(4)][e]
R(C,H)	1.100	1.098 [1.072(2)][c]	1.101	1.100 [1.094][d]	1.104	1.104 [1.082(4), 1.103(2)][e]
R(M,M)	2.413	2.400 [2.591(9)][c]	3.015	3.020 [2.97−3.17][d]	3.761	3.746
R(C,C)	3.641	3.608 [3.621(6)][c]	4.188	4.162	4.689	4.591
∠HCH	103.02	103.62 [108.2(2)][c]	102.64	104.26 [106.2][d]	102.58	103.32 [104.8(2), 105.8(2)][e]
∠CMCM	23.23	24.06	18.95	18.49	12.69	11.70
α	109.36	109.87	106.50	106.18	101.70	100.87
β	66.14	65.31	70.46	70.93	76.92	77.95

[a] α and *β* angles correspond to those in Figure 4. [b] Experimental values in brackets. [c] Experimental neutron diffraction, 1.5 K.[14] [d] Experimental neutron + synchrotron diffraction, 1.5 K.[15] [e] Experimental neutron diffraction, 1.35 K, for the CD_3K_3 entities in the $(CD_3K)_6$ unit cell of the methylpotassium crystal.[13]

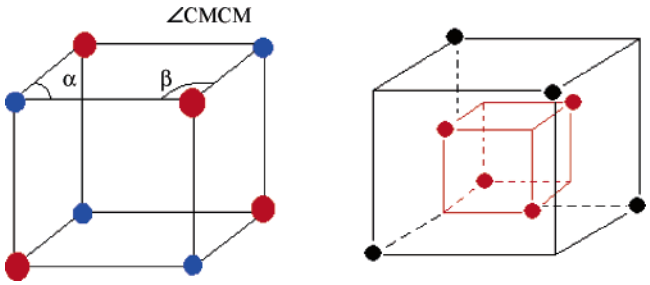

Figure 4. Schematic vision of the methylalkalimetal tetramers geometry. The angles α, *β* and the dihedral ∠CMCM are shown.

TABLE 6: HF/6-311G Atomic Populations (N), Atomic Charges (q), Localization Indices (*λ*), Localization Percentages (%*λ*), and Delocalization Indices (*δ*) Obtained from the Atoms in Molecules Analysis for the Most Stable Methylalkalimetal Tetramers. Units Are Electrons**

molecule	atom	*N*	*q*	*λ*	%*λ*	pair	*δ*(A,B)
$(CH_3Li)_4$	C	6.533	−0.533	4.763	72.9	C,Li	0.071
ecl	Li	2.105	0.895	1.972	93.7	C,H	1.043
	H	1.121	−0.121	0.527	47.0	H,H′	0.059
						C,C′	0.056
						Li,Li′	0.002
$(CH_3Na)_4$	C	6.443	−0.443	4.701	73.0	C,Na	0.088
ecl	Na	10.122	0.878	9.953	98.3	C,H	1.046
	H	1.145	−0.145	0.545	47.7	H,H′	0.063
						C,C′	0.023
						Na,Na′	0.003
$(CH_3K)_4$	C	6.405	−0.495	4.657	72.7	C,K	0.109
stg	K	18.116	0.884	17.908	98.9	C,H	1.047
	H	1.160	−0.160	0.556	48.0	H,H′	0.065
						C,C′	0.007
						K,K′	0.004

AIM Analysis. AIM and ELF analyses provide very similar results for the eclipsed and staggered conformations of the methylalkalimetal tetramers. For this reason, the analysis will be focused on the most stable conformation for each species (eclipsed for Li and Na, and staggered for K, which are minima in their respective potential energy surfaces). The values obtained from the AIM analysis of atomic populations, atomic charges, LIs, localization percentages, and DIs of these species are listed in Table 6. The values corresponding to the least stable conformations can be found in the Supporting Information.

With respect to the monomers, the metal charge is slightly lower by 0.02 e in the methyllithium tetramer, whereas for methylsodium and -potassium tetramers the metal charges are larger by 0.08 and 0.05 e, respectively. As a result, the three tetramers have almost the same metal charge. Now, the reduction of the np_σ AO contribution in the bonding when going from Li to Na is less relevant, as far as the metal charge is concerned, because the np_σ admixture to the metal cluster orbitals makes them point inward into the metal tetrahedron, and the charge collected by the resulting metal orbitals is almost entirely accommodated on the metal cluster.

Table 3 also contains the values for the tetramers of the $\rho(\mathbf{r}_{bcp})$, $\nabla^2\rho(\mathbf{r}_{bcp})$, $H(\mathbf{r}_{bcp})$, and $|\lambda_1|/\lambda_3$ parameters. As it can be seen from Table 3, the values of $\rho(\mathbf{r}_{bcp})$, $\nabla^2\rho(\mathbf{r}_{bcp})$, and $|\lambda_1|/\lambda_3$ are slightly lower for the tetramers than for the monomers, but they follow the same tendency: $|\lambda_1|/\lambda_3 < 1$, $\rho(\mathbf{r}_{bcp})$ small, $\nabla^2\rho(\mathbf{r}_{bcp}) > 0$, and $H(\mathbf{r}_{bcp}) > 0$, thus indicating clearly the ionic nature of the C−M bond. As stated for the monomers, the ionic character of this bond regularly increases from Li to K according to $\rho(\mathbf{r}_{bcp})$ and $\nabla^2\rho(\mathbf{r}_{bcp})$ values. LIs for the metal atom in the tetramers (Table 6) are slightly lower by 0.01 (Li) to 0.05 (K) e in comparison with the corresponding monomers. In line with this, the localization percentages (%*λ*) for the tetramers are almost identical to those of the corresponding monomers and reveal an increase of ionicity from methyllithium to methylpotassium. *δ*(C,M) values for the tetramers are approximately reduced to one-third as compared to those found for the corresponding monomers, because now the metal atom interacts with three equivalent C atoms. These low DIs are characteristic of ionic interactions.[43] The increase in DIs when going from Li to K fits with the reduction of LIs in the same direction. The *δ*(C,H) values are only slightly inferior to those of the monomers (∼1.04 e). It is also worth noting the *δ*(C,C′) values, which decrease when going from Li (0.056), to Na (0.023), and to K (0.007), especially due to an increase in the C−C′ distance. It is also interesting to mention the *δ*(M,M′) values that are almost imperceptible (0.002−0.004 e), showing that there is no electronic delocalization between the metal atoms.

On the other hand, Figure 5 depicts the different critical points found for the three tetramers studied in their most stable conformation, including bond, ring, and cage critical points. These representations should help us to characterize the different bonds present in the tetramers. According to AIM theory, the criterion for assigning bonding between two atoms is the existence of a bond critical point connecting them by a gradient path.[54,55] Note, however, that this is an unproven premise.[56−58] For the methyllithium tetramer, either in the eclipsed or

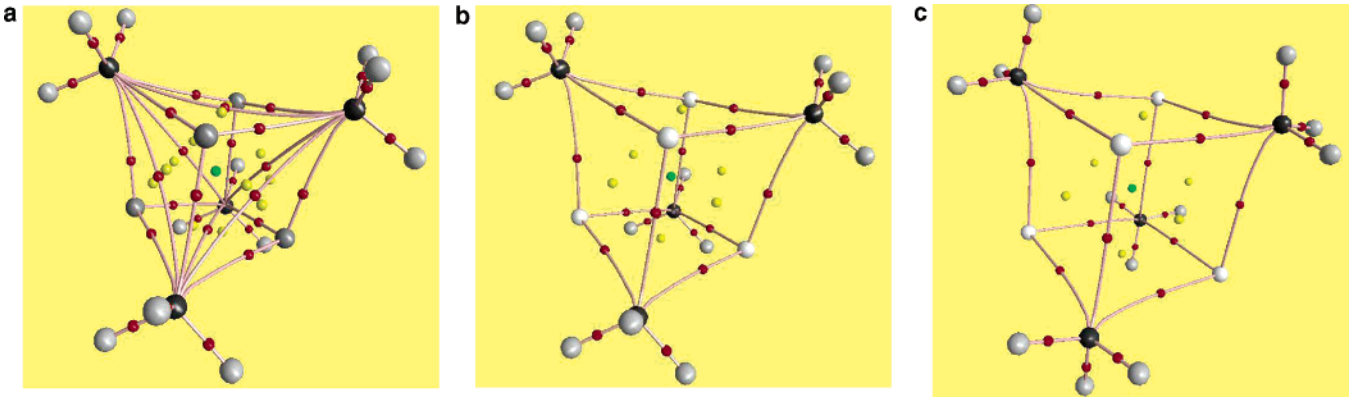

Figure 5. AIM representation of the methylalkalimetal tetramers $(CH_3M)_4$ with M = Li (a), Na (b), and K (c) in eclipsed conformation for Li and Na, and in staggered conformation for K, including the bond (red), ring (yellow), and cage (green) critical points. M is depicted in white, while hydrogen and carbons are colored in gray and black.

TABLE 7: HF/6-311G ELF Values at Attractors (η), Basin Populations ($N(\Omega_i)$), Standard Deviations ($\sigma^2(\Omega_i)$), Relative Fluctuations ($\lambda_F(\Omega_i)$), and Contributions of the Other Basins (%) to $\sigma^2(\Omega_i)$, Obtained for the Most Stable Methylalkalimetal Tetramers**

molecule	Ω	η	$N(\Omega_i)$	$\sigma^2(\Omega_i)$	$\lambda_F(\Omega_i)$	contribution analysis
$(CH_3Li)_4$	C(C)	0.16	2.09	0.25	0.12	28%V(C), 24%V(C,H$_i$)
ecl	C(Li)	0.03	2.03	0.10	0.05	22%V(C), 11%V(C,H$_i$)
	V(C,H$_i$)	0.79	1.95	0.68	0.34	35%V(C), 27%V(C,H$_i$), 9%C(C)
	V(C)	0.79	2.03	0.95	0.47	26%V(C,H$_i$)
$(CH_3Na)_4$	C(C)	0.23	2.09	0.25	0.12	28%V(C), 24%V(C,H$_i$)
ecl	C(Na)	0.03	10.01	0.14	0.01	25%V(C), 8%V(C,H$_i$)
	V(C,H$_i$)	0.75	1.96	0.67	0.34	36%V(C), 27%V(C,H$_i$), 10%C(C)
	V(C)	0.75	2.00	0.93	0.46	26%V(C,H$_i$)
$(CH_3K)_4$	C(C)	0.16	2.09	0.24	0.12	28%V(C), 24%V(C,H$_i$)
stg	C(K)	0.05	18.02	0.19	0.01	19%V(C), 14%V(C,H$_i$)
	V(C,H$_i$)	0.79	1.97	0.68	0.34	34%V(C), 26%V(C,H$_i$), 14%C(C)
	V(C)	0.79	1.96	0.92	0.47	26%V(C,H$_i$)

staggered conformations, it can be seen that each carbon atom is bound to three hydrogen atoms, to the other three carbon atoms (despite the separation of more than 3.5 Å) and at the same time to the three lithium atoms closest to it, which constitute the face of the metal cluster that the methyl group is pointing toward. Thus, taking into consideration the bond critical points, this situation would mean that each carbon is forming nine chemical bonds. A cage critical point in the center of the distorted cube is also observed, and on each face of the cube we find two ring critical points, corresponding to C−Li−C coupling. This unexpected topological description, observed previously at the HF/3-21G level,[17] cannot be attributed to an artifact deriving from a too low level of quantum chemical theory since it is reproduced using the correlated B3LYP and MP2 methods with the 6-311++G(3df,3pd) basis set. A similar behavior to that found for the methyllithium tetramer has been previously put forth in the interaction of Mn[55] and Ti[59] with the carbons of a cyclopentadienyl ring and in the metallocenes of Al^+, Fe, and Ge.[34] According to Bader et al.,[55] the bonding of a metal atom to an unsaturated ring is not well represented in terms of a set of individual bond paths, but rather by a bonded cone of density. However, there are also a number of authors that consider that the conjecture that a bond path between two atoms in an equilibrium structure implies the presence of a chemical bond is not valid.[57,60] This latter view is supported by the presence of bond paths between anions in ionic crystals[61] and in many H···H repulsive interactions in polycyclic aromatic hydrocarbons (PAHs) such as kekulene, phenanthrene, chrysene, or benzanthracene[56,60,62] and other sterically overcrowded molecules.[63] In our case, DIs help in the aim of clarifying whether there is C−C bonding in these systems. Indeed, the low δ(C,C′) values clearly point out that there is no direct C−C bonding.[64] Less clear is the situation for the M−M bonding, since metallic bonding is usually associated with low DIs.[43]

For the methylsodium tetramer, we find that each sodium atom is bound to the three closest carbon atoms, and each carbon atom is bound to the three hydrogen atoms of the corresponding methyl group, together to the three closest Na atoms. However there is no bond critical point between the carbon atoms for this structure. We also observe a cage critical point, but now there is only one ring critical point on each face of the cube, which is less distorted with respect to the Li one. The methylpotassium tetramer, with the less distorted cube structure, also presents the same critical points. Thus, each carbon atom in Na and K tetramers is connected to six atoms according to the AIM analysis (cf. Figures 5b and 5c).

ELF Analysis. Table 7 contains the most important parameters obtained from this analysis for the three tetramers in their most stable conformation. The Supporting Information contains the results for the least stable conformation.

As found in the AIM analysis, ELF values for the monomers and the tetramers do not differ much. First, as it can be seen from Table 7, the study has defined the same basins as for the monomers: C(C), C(M), V(C,H$_i$), and V(C). This proves that there is no new interaction when going from the monomer to the tetramer structure, i.e. new disynaptic attractors as V(C,M), V(C,C′), or V(M,M′).

Focusing on the basin population values for the tetramers, C(C) basins are slightly more populated by 0.02−0.04 e than in the monomers. The same happens for the population of C(M) basin when M = Li by 0.03 e, whereas for M = Na and K the population decreases by 0.03 and 0.04 e, respectively. With respect to the disynaptic basins, the V(C,H$_i$) populations are also lower by 0.02−0.03 e in the tetramers than in the

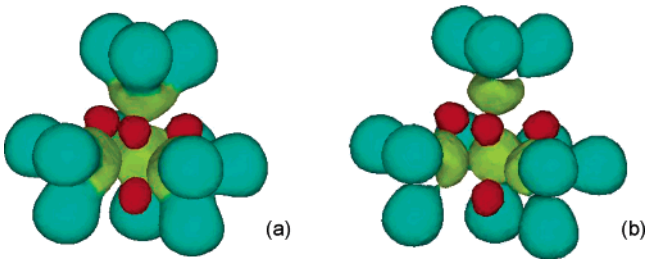

Figure 6. ELF isosurface of the methyllithium tetramer in its eclipsed conformation with η values of 0.60 (a) and 0.80 (b). The color scale code used for the localization domain is as follows: core, red; valence protonated, green; valence tetrasynaptic, yellow.

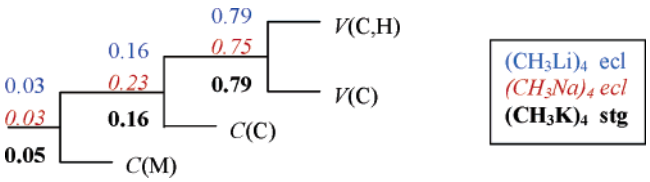

Figure 7. Localization domain reduction tree-diagram of methylalkalimetal tetramers $(CH_3M)_4$ with M = Li, Na, and K.

monomers. Meanwhile, V(C) basin populations are those that undergo the most important changes when forming the tetramer, increasing by 0.02 (Li) − 0.08 (Na, K) e, and at the same time equalizing their populations (2.00−2.03 e), thus reinforcing the ionic character with respect to the monomers. Less important are the changes on the relative fluctuation parameter ($\lambda_F(\Omega_i)$), which is kept almost unaltered for the three first basins, while only V(C) is increased by 0.05, thus showing a higher electronic delocalization for this basin. The same happens for the contribution analysis results also enclosed in Table 7, which present very similar values to those found in the monomers.

If we look at the ELF isosurface plots depicted in Figure 6 for the methyllithium tetramer in its eclipsed conformation, more valuable information can be obtained. ELF isosurface plots for the other systems studied have not been enclosed as they are almost visually equivalent to these ones. First, the above commented four different basins can be easily distinguished, especially in the plot with ELF = 0.80. In this case, it is clearly seen how the monosynaptic V(C) basin does not point to any of the three closest monosynaptic C(Li) basins, but to the center of a triangular face of the tetrahedron defined by the Li_4 unit. The V(C) basin does not lie in the line connecting the cores, but the line connecting the C(C) and the center of the three C(Li), pretty close to the core basin of C, and circumscribing it (see Figure 6a). So this bonding situation can also be described as ionic, like for the monomers. Each methyl group ionically interacts with one face of the tetrahedron created with three Li atoms. This ELF picture is very similar to that found for Li_4H_4, in which each H localizes one valence electron of the Li atoms.[65] The same is true for the other metals and different conformers analyzed in the present work.

Again, the bifurcation analysis scheme (see Figure 7) provides a hierarchy that is consistent with the relative fluctuation values. For the tetramers, the C(M) basin is partitioned earlier, $\eta \approx 0.03-0.05$, than for the monomers, indicating a minor increase in ionicity when going from the monomers to the tetramers, but C(C) basin is partitioned later with $\eta \approx 0.16-0.23$. And again, it is not until $\eta \approx 0.75-0.80$ that the valence basin is split into $V(C,H_i)$ and V(C) basins. So, also for this analysis, the similarity of the results with respect to those obtained by the monomers makes us attribute a noticeable ionic character to the C−M interaction in methylalkalimetal tetramers.

4. Conclusions

The AIM and ELF topological approaches partially agree but also show significant divergences in the description of the bonding in methylalkalimetals $(CH_3M)_n$ with M = Li, Na, K, n = 1, 4. They agree that the C−M bond in these compounds is highly polar. However, whereas AIM indicates that tetramerization of CH_3M slightly reduces the polarity, ELF suggests the opposite.

More importantly, and also more strikingly, AIM yields nonavalent carbons in tetramethyllithium. According to AIM, the carbon atoms in this methylalkalimetal have three individual bonds to the three closest hydrogen atoms, three individual bonds to the three closest metal atoms, and three individual bonds to the three closest carbon atoms. At variance, ELF yields tetravalent carbon atoms that form three covalent bonds with their hydrogens plus one polar bond with a triangular face of the central metal cluster. This ELF topological result fits well with the bonding picture that emerges from quantitative Kohn−Sham molecular orbital analyses.[16]

Acknowledgment. Financial help has been furnished by the Spanish MEC Project No. CTQ2005-08797-C02-01/BQU, The Netherlands Organization for Scientific Research (NWO), and the HPC-Europa as well as the Training and Mobility of Researchers (TMR) programs of the European Union. E.M. and J.P. thank the Ministerio de Educación y Ciencia for the doctoral fellowship no. AP2002-0581 and the DURSI for the postdoctoral fellowship 2004BE00028, respectively. Excellent service by the Stichting Academisch Rekencentrum Amsterdam (SARA) and the Centre de Supercomputació de Catalunya (CESCA) is gratefully acknowledged.

Supporting Information Available: Tables containing the AIM and ELF results for the least stable $(CH_3M)_4$ (M = Li, Na, and K) conformers. This material is available free of charge via the Internet at http://pubs.acs.org.

References and Notes

(1) Elschenbroich, C.; Salzer, A. *Organometallics. A concise introduction*, 2nd ed.; VCH: Weinheim, 1992; March, J. *Advanced Organic Chemistry*, 4th ed.; Wiley-Interscience: New York, 1992; Carey, F. A.; Sundberg, R. J. *Advanced Organic Chemistry, Part A*; Plenum Press: New York, 1984; Collman, J. P.; Hegedus, L. S.; Norton, J. R.; Finke, R. G. *Principles and Applications of Organotransition Metal* Chemistry; University Science Books: Mill Valley, 1987; Knochel, P.; Dohle, W.; Gommermann, N.; Kneisel, F. F.; Kopp, F.; Korn, T.; Sapountzis, I.; Vu, V. A. *Angew. Chem., Int. Ed.* **2003**, *42*, 4302.

(2) Schleyer, P. v. R. *Pure Appl. Chem.* **1983**, *55*, 355; Setzner, W. N.; Schleyer, P. v. R. *Adv. Organomet. Chem.* **1985**, *24*, 354.

(3) Streitwieser, A., Jr.; Williams, J. E., Jr.; Alexandratos, S.; McKelvey, J. M. *J. Am. Chem. Soc.* **1976**, *98*, 4778.

(4) Streitwieser, A., Jr. *J. Organomet. Chem.* **1978**, *156*, 1.

(5) Lambert, C.; Kaupp, M.; Schleyer, P. v. R. *Organometallics* **1993**, *12*, 853; Lambert, C.; Schleyer, P. v. R. *Angew. Chem., Int. Ed. Engl.* **1994**, *33*, 1129; Bauer, W.; Winchester, W. R.; Schleyer, P. v. R. *Organometallics* **1987**, *6*, 2371; Fressigné, C.; Maddaluno, J.; Giessner-Prettre, C. *J. Chem. Soc., Perkin Trans. 2* **1999**, 2197; Schiffer, H.; Ahlrichs, R. *Chem. Phys. Lett.* **1986**, *124*, 172.

(6) Ponec, R.; Roithová, J.; Gironés, X.; Lain, L.; Torre, A.; Bochicchio, R. *J. Phys. Chem. A* **2002**, *106*, 1019.

(7) Kremer, T.; Harder, S.; Junge, M.; Schleyer, P. v. R. *Organometallics* **1996**, *15*, 585; Tyerman, S. C.; Corlett, G. K.; Ellis, A. M.; Claxton, T. A. *J. Mol. Struct. (THEOCHEM)* **1996**, *364*, 107; El-Nahas, A. M.; Schleyer, P. v. R. *J. Comput. Chem.* **1994**, *15*, 596; Wiberg, K.; Breneman, C. M. *J. Am. Chem. Soc.* **1990**, *112*, 8765.

(8) Breidung, J.; Thiel, W. *J. Mol. Struct. (THEOCHEM)* **2001**, *599*, 239; Scalmani, G.; Brédas, J. L. *J.* Chem. Phys. **2000**, *112*, 1178.

(9) Kaufmann, E.; Raghavachari, K.; Reed, A. E.; Schleyer, P. v. R. *Organometallics* **1988**, *7*, 1597; Kwon, O.; Sevin, F.; McKee, M. L. *J. Phys. Chem. A* **2001**, *105*, 913.

(10) Grotjahn, D. B.; Pesch, T. C.; Brewster, M. A.; Ziurys, L. M. *J. Am. Chem. Soc.* **2000**, *122*, 4735.

(11) Grotjahn, D. B.; Apponi, A. J.; Brewster, M. A.; Xin, J.; Ziurys, L. M. *Angew. Chem. Int. Ed.* **1998**, *37*, 2678; Andrews, L. *J. Chem. Phys.* **1967**, *47*, 4834; Weiss, E.; Hencken, G. *J. Organomet. Chem.* **1970**, *21*, 265.

(12) Grotjahn, D. B.; Pesch, T. C.; Xin, J.; Ziurys, L. M. *J. Am. Chem. Soc.* **1997**, *119*, 12368.

(13) Weiss, E.; Lambertsen, T.; Schubert, B.; Cockcroft, J. K. *J. Organomet. Chem.* **1988**, *358*, 1.

(14) Weiss, E.; Lambertsen, T.; Schubert, B.; Cockcroft, J. K.; Wiedenmann, A. *Chem. Ber.* **1990**, *123*, 79.

(15) Weiss, E.; Corbelin, S.; Cockcroft, J. K.; Fitch, A. N. *Angew. Chem., Int. Ed. Engl.* **1990**, *29*, 650; Weiss, E.; Corbelin, S.; Cockcroft, J. K.; Fitch, A. N. *Chem. Ber.* **1990**, *123*, 1629.

(16) Bickelhaupt, F. M.; van Eikema Hommes, N. J. R.; Fonseca Guerra, C.; Baerends, E. J. *Organometallics* **1996**, *15*, 2923.

(17) Ritchie, J. P.; Bachrach, S. M. *J. Am. Chem. Soc.* **1987**, *109*, 5909.

(18) Hiberty, P. C.; Cooper, D. L. *J. Mol. Struct. (THEOCHEM)* **1988**, *169*, 437; Cioslowski, J. *J. Am. Chem. Soc.* **1989**, *111*, 8333.

(19) Vidal, I.; Melchor, S.; Dobado, J. A. *J. Phys. Chem. A* **2005**, *109*, 7500.

(20) Cooper, D. L.; Gerratt, J.; Karadakov, P. B.; Raimondi, M. *J. Chem. Soc., Faraday Trans.* **1995**, *91*, 3363.

(21) Bushby, R. J.; Steel, H. L. *J. Organomet. Chem.* **1987**, *336*, C25; Bushby, R. J.; Steel, H. L. *J. Chem. Soc., Perkin Trans. 2* **1990**, 1143.

(22) Günter, H.; Moskau, D.; Bast, P.; Schmalz, D. *Angew. Chem., Int. Ed. Engl.* **1987**, *26*, 1212; Bauer, W.; Schleyer, P. v. R. *Adv. Carbanion Chem.* **1992**, *1*, 89; Bauer, W. *Lithium Chemistry*; Wiley-Interscience: New York, 1995; Fraenkel, G.; Martin, K. V. *J. Am. Chem. Soc.* **1995**, *117*, 10336.

(23) Ebel, H. F. *Tetrahedron* **1965**, *21*, 699; Armstrong, D. R.; Perkins, P. G. *Coord. Chem.Rev.* **1981**, *38*, 139.

(24) Sapse, A. M.; Raghavachari, K.; Schleyer, P. v. R.; Kaufmann, E. *J. Am. Chem. Soc.* **1985**, *107*, 6483.

(25) Hirshfeld, F. L. *Theor. Chim. Acta* **1977**, *44*, 129.

(26) Fonseca Guerra, C.; Handgraaf, J.-W.; Baerends, E. J.; Bickelhaupt, F. M. *J. Comput. Chem.* **2004**, *25*, 189.

(27) Bickelhaupt, F. M.; Solà, M.; Fonseca Guerra, C. *J. Mol. Model.* **2006**, in press.

(28) Bader, R. F. W. *Atoms in Molecules: A Quantum Theory*; Clarendon: Oxford, 1990.

(29) Savin, A.; Nesper, R.; Wengert, S.; Fässler, T. *Angew. Chem., Int. Ed. Engl.* **1997**, *36*, 1808.

(30) Bader, R. F. W.; Stephens, M. E. *J. Am. Chem. Soc.* **1975**, *97*, 7391.

(31) Fradera, X.; Austen, M. A.; Bader, R. F. W. *J. Phys. Chem. A* **1999**, *103*, 304; Fradera, X.; Poater, J.; Simon, S.; Duran, M.; Solà, M. *Theor. Chem. Acc.* **2002**, *108*, 214.

(32) Bader, R. F. W. *Acc. Chem. Res.* **1985**, *18*, 9.

(33) Bader, R. F. W. *Chem. Rev.* **1991**, *91*, 893.

(34) Cortés-Guzmán, F.; Bader, R. F. W. *Coord. Chem. Rev.* **2005**, *249*, 633.

(35) Becke, A. D.; Edgecombe, K. E. *J. Chem. Phys.* **1990**, *92*, 5397.

(36) Noury, S.; Colonna, A.; Savin, A. *J. Mol. Struct. (THEOCHEM)* **1998**, *450*, 59.

(37) Savin, A.; Silvi, B.; Colonna, F. *Can. J. Chem.* **1996**, *74*, 1088.

(38) Fourré, I.; Silvi, B.; Sevin, A.; Chevreau, H. *J. Phys. Chem. A* **2002**, *106*, 2561.

(39) Bader, R. F. W.; Stephens, M. E. *Chem. Phys. Lett.* **1974**, *26*, 445.

(40) Poater, J.; Solà, M.; Duran, M.; Fradera, X. *Theor. Chem. Acc.* **2002**, *107*, 362.

(41) Jansen, G.; Schubart, M.; Findeis, B.; Gade, L. H.; Scowen, I. J.; McPartlin, M. *J. Am. Chem. Soc.* **1998**, *120*, 7239; Raub, S.; Jansen, G. *Theor. Chem. Acc.* **2001**, *106*, 223; Poater, J.; Duran, M.; Solà, M.; Silvi, B. *Chem. Rev.* **2005**, *105*, 3911.

(42) Bader, R. F. W.; Slee, T. S.; Cremer, D.; Kraka, E. *J. Am. Chem. Soc.* **1983**, *105*, 5061; Bader, R. F. W.; Macdougall, P. J. *J. Am. Chem. Soc.* **1985**, *107*, 6788; Solà, M.; Mestres, J.; Carbó, R.; Duran, M. *J. Chem. Phys.* **1996**, *104*, 636.

(43) Macchi, P.; Sironi, A. *Coord. Chem. Rev.* **2003**, *238*−*239*, 383.

(44) Frisch, M. J.; Trucks, G. W.; Schlegel, H. B.; Scuseria, G. E.; Robb, M. A.; Cheeseman, J. R.; Zakrzewski, V. G.; Montgomery, J. A.; Stratmann, R. E.; Burant, J. C.; Dapprich, S.; Millam, J. M.; Daniels, A. D.; Kudin, K. N.; Strain, M. C.; Farkas, O.; Tomasi, J.; Barone, V.; Cossi, M.; Cammi, R.; Mennucci, B.; Pomelli, C.; Adamo, C.; Clifford, S.; Ochterski, J.; Petersson, G. A.; Ayala, P. Y.; Cui, Q.; Morokuma, K.; Salvador, P.; Dannenberg, J. J.; Malick, D. K.; Rabuck, A. D.; Raghavachari, K.; Foresman, J. B.; Cioslowski, J.; Ortiz, J. V.; Baboul, A. G.; Stefanov, B. B.; Liu, G.; Liashenko, A.; Piskorz, P.; Komaromi, I.; Gomperts, R.; Martin, R. L.; Fox, D. J.; Keith, T.; Al-Laham, M.; Peng, C.; Nanayakkara, A.; Challacombe, M.; Gill, P. M. W.; Johnson, B. G.; Chen, W.; Wong, M. W.; Andres, J. L.; Gonzalez, R.; Head-Gordon, M.; Replogle, E. S.; Pople, J. A. Gaussian 98; Gaussian 98, rev. A11: Pittsburgh, PA, 1998.

(45) Biegler-König, F. W.; Bader, R. F. W.; Tang, T.-H. *J. Comput. Chem.* **1982**, *3*, 317.

(46) Wang, Y. G.; Werstiuk, N. H. *J. Comput. Chem.* **2003**, *24*, 379.

(47) Biegler-König, F.; Schonbohm, J.; Bayles, D. *J. Comput. Chem.* **2001**, *22*, 545.

(48) Noury, S.; Krokidis, X.; Fuster, F.; Silvi, B. TopMod package; TopMod package: Paris, 1997.

(49) Hibbard, B.; Kellum, J.; Paul, B. Vis5d 5.1, Visualization Project; Vis5d 5.1, Visualization Project: University of Wisconsin-Madison Space Science and Engineering Center (SSEC), 1990; Hibbard, B.; Santek, D. *Proc. IEEE* **1990**, *129*, 28.

(50) Lambert, C.; Kaupp, M.; Schleyer, P. v. R. *Organometallics* **1993**, *12*, 853.

(51) Silvi, B.; Savin, A. *Nature* **1994**, *371*, 683.

(52) Joubert, L.; Picard, G.; Silvi, B.; Fuster, F. *J. Mol. Struct. (THEOCHEM)* **1999**, *463*, 75; Lundell, J.; Panek, J.; Latajka, Z. *Chem. Phys. Lett.* **2001**, *348*, 147; Savin, A.; Becke, A. D.; Flad, J.; Nesper, R.; Preuss, H.; von Schnering, H. G. *Angew. Chem., Int. Ed. Engl.* **1991**, *30*, 409; Gomes, J. R. B.; Illas, F.; Silvi, B. *Chem. Phys. Lett.* **2004**, *388*, 132.

(53) Mierzwicki, K.; Berski, S.; Latajka, Z. *Chem. Phys. Lett.* **2000**, *331*, 538.

(54) Bader, R. F. W. *J. Phys. Chem. A* **1998**, *102*, 7314.

(55) Bader, R. F. W.; Matta, C. F.; Cortés-Guzmán, F. *Organometallics* **2004**, *23*, 6253.

(56) Cioslowski, J.; Mixon, S. T. *J. Am. Chem. Soc.* **1992**, *114*, 4382.

(57) Haaland, A.; Shorokhov, D. J.; Tverdova, N. V. *Chem. Eur. J.* **2004**, *10*, 4416.

(58) Poater, J.; Solà, M.; Bickelhaupt, F. M. *Chem. Eur. J.* **2006**, *12*, 2889.

(59) Bader, R. F. W.; Matta, C. F. *Inorg. Chem.* **2001**, *40*, 5603.

(60) Cioslowski, J.; Mixon, S. T. *Can. J. Chem.* **1992**, *70*, 443.

(61) Martín Pendás, A.; Costales, A.; Luaña, V. *Phys. Rev. B* **1997**, *55*, 4275; Abramov, Y. A. *J. Phys.* Chem. A **1997**, *101*, 5725; Tsirelson, V.; Abramov, Y. A.; Zavodnik, V.; Stash, A.; Belokoneva, E.; Stahn, J.; Pietsch, U.; Feil, D. *Struct. Chem.* **1998**, *9*, 249; Tsirelson, V. G.; Avilov, A. S.; Lepeshov, G. G.; Kulygin, A. K.; Pietsch, U.; Spence, J. C. H. *J. Phys. Chem. B* **2001**, *105*, 5068.

(62) Cioslowski, J.; Mixon, S. T.; Edwards, W. D. *J. Am. Chem. Soc.* **1991**, *113*, 1083; Visser, R.; Bickelhaupt, F. M.; Poater, J.; Solà, M. **2006**, submitted for publication.

(63) Cioslowski, J.; Edgington, L.; Stefanov, B. B. *J. Am. Chem. Soc.* **1995**, *117*, 10381.

(64) Glukhovtsev, M. N.; Schleyer, P. v. R.; Stein, A. *J. Phys. Chem.* **1993**, *97*, 5541.

(65) Fuentealba, P.; Savin, A. *J. Phys. Chem. A* **2001**, *105*, 11531.